Epitaxial Templating of C_{60} with a Molecular Monolayer

L. A. Rochford[a], T. S. Jones[a] and C. B. Nielsen[b]*

a. Department of Chemistry, University of Warwick, Gibbet Hill Road, Coventry, CV4 7AL, UK.

b. Materials Research Institute and School of Biological and Chemical Sciences, Queen Mary University of London, Mile End Road, London E1 4NS, United Kingdom

AUTHOR INFORMATION

Corresponding Author

* E-mail: luke.rochford@warwick.ac.uk

Commensurate epitaxial monolayers of truxenone on Cu (111) were employed to template the growth of monolayer and bilayer C60. Through the combination of STM imaging and LEED analysis we have demonstrated that C60 forms a commensurate 8x8 overlayer on truxenone/Cu (111). Bilayers of C60 retain the 8x8 periodicity of templated monolayers and although Kagome lattice arrangements are observed these are explained with combinations of 8x8 symmetry

TOC GRAPHICS

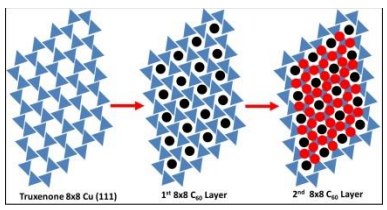

KEYWORDS LEED, STM, Truxenone, Fullerene, Surfaces and Interfaces

The ability to control the structure of crystalline layers of organic semiconductors is hugely attractive in the field of organic electronics[1–4]. By modifying the crystal structure of organic materials structure-property relationships can be exploited for fundamental understanding and device applications[3,5]. A concerted research effort has been directed into using open-pored low dimensional organic frameworks to control the earliest stages of crystallisation in organic semiconductors – most notably buckminsterfullerene (C_{60}) in ultra-high vacuum and at solid/liquid interfaces [6–15]. Here we present the use of a commensurate epitaxial template to direct the growth of commensurate epitaxial C_{60} layers. This strategy imparts the structural symmetry and in-plane structural order of the substrate into the molecular template and subsequent C_{60} layers. Our recent work has demonstrated that truxenones, a family of three-fold symmetric organic semiconductors, self-assemble to form epitaxial open-pored structures on Cu (111), a highly unusual observation in semiconducting organic molecules[16,17]. Combining truxenone and Cu (111) allows the creation of model surfaces to understand directed assembly behaviour while employing a material system which is relevant for high performance device applications such as organic photovoltaics[18–20]. Through a combination of STM (Scanning tunnelling microscopy) and LEED (Low energy electron diffraction) we demonstrate that a modified C_{60} layer forms within the pores of the truxenone network, exhibiting an 8x8 unit mesh

with respect to the underlying Cu(111) surface. A second C_{60} layer is also characterised and corresponds to three additional 8x8 unit meshes laterally translated with respect to the substrate. The combination of fundamental hexagonal symmetry is used to explain ostensibly complex surface symmetry (that of a Kagome lattice). These structural conclusions are unambiguously demonstrated by considering both real space visualisation (STM) and reciprocal space structural analysis (LEED).

Our recent work has established that truxenone molecules (Figure 1(a) inset) form a commensurate 8x8 structure on the Cu (111) surface at room temperature[16,17]. STM images of small (a) and large (c) areas of the truxenone/Cu (111) evaporated on to clean Cu (111) in ultra-high vacuum (UHV)‡ are shown in Figure 1 along with a LEED pattern (b) of the same surface recorded at 13 eV. This arrangement of molecules effectively creates an ordered array of open pores, approximately 0.7 nm in diameter and exactly 2.04 nm apart, aligned with the principal lattice vectors of the substrate.

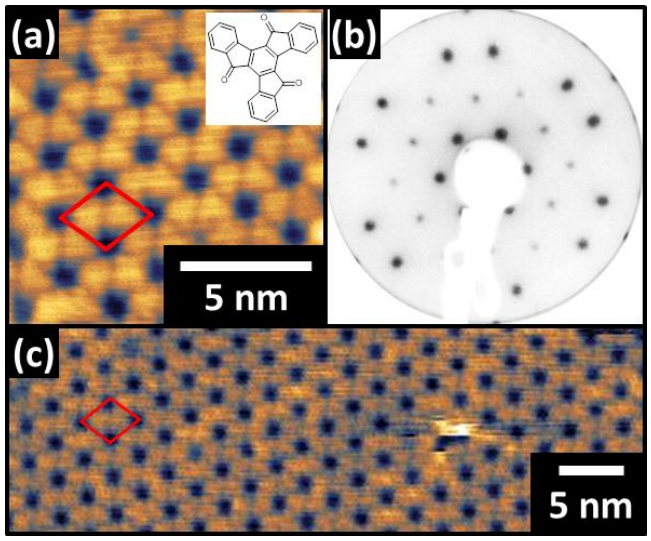

Figure 1 – STM images (Vs=-1.25V, It=65pA) of small (a) and large (c) areas of 8x8 truxenone/Cu (111) (unit cells marked by red rhombuses) along with a LEED pattern (b) at 13eV. The inset in panel (a) shows the chemical structure of the truxenone molecule.

The pro-chiral nature of truxenone means that surface induced enantiomers are possible when supported by a surface, but these cannot be discriminated between in our experiments[16]. Consequently, no obvious 'handedness' is observed in the supramolecular arrangement creating the pores although an achiral surface cannot be established[21,22]. A proposed packing schematic with potential hydrogen bonds indicated is included in the supporting information (Figure S1).

C_{60} was sequentially evaporated on to this porous mesh and probed by scanning tunnelling microscopy (STM) and low energy electron diffraction (LEED). The STM image in Figure 2(a) demonstrates that C_{60} molecules form a hexagonal lattice on top of the truxenone layer. Each 'pore' of the 8x8 truxenone/Cu (111) mesh accommodates a single C_{60} molecule, leading to the formation of a C_{60} layer with the same periodicity as the underlying 8x8 mesh. The LEED pattern from the same surface (Fig. 2(b)) confirms that 8x8 symmetry is preserved on the addition of C_{60}. As the C_{60} layer also exhibits 8x8 registry with the underlying Cu (111) the translational and rotation symmetry of the substrate was preserved. In the same STM image (Fig 2(b)) brighter islands can be observed which may correspond to bilayer growth of C_{60}. The

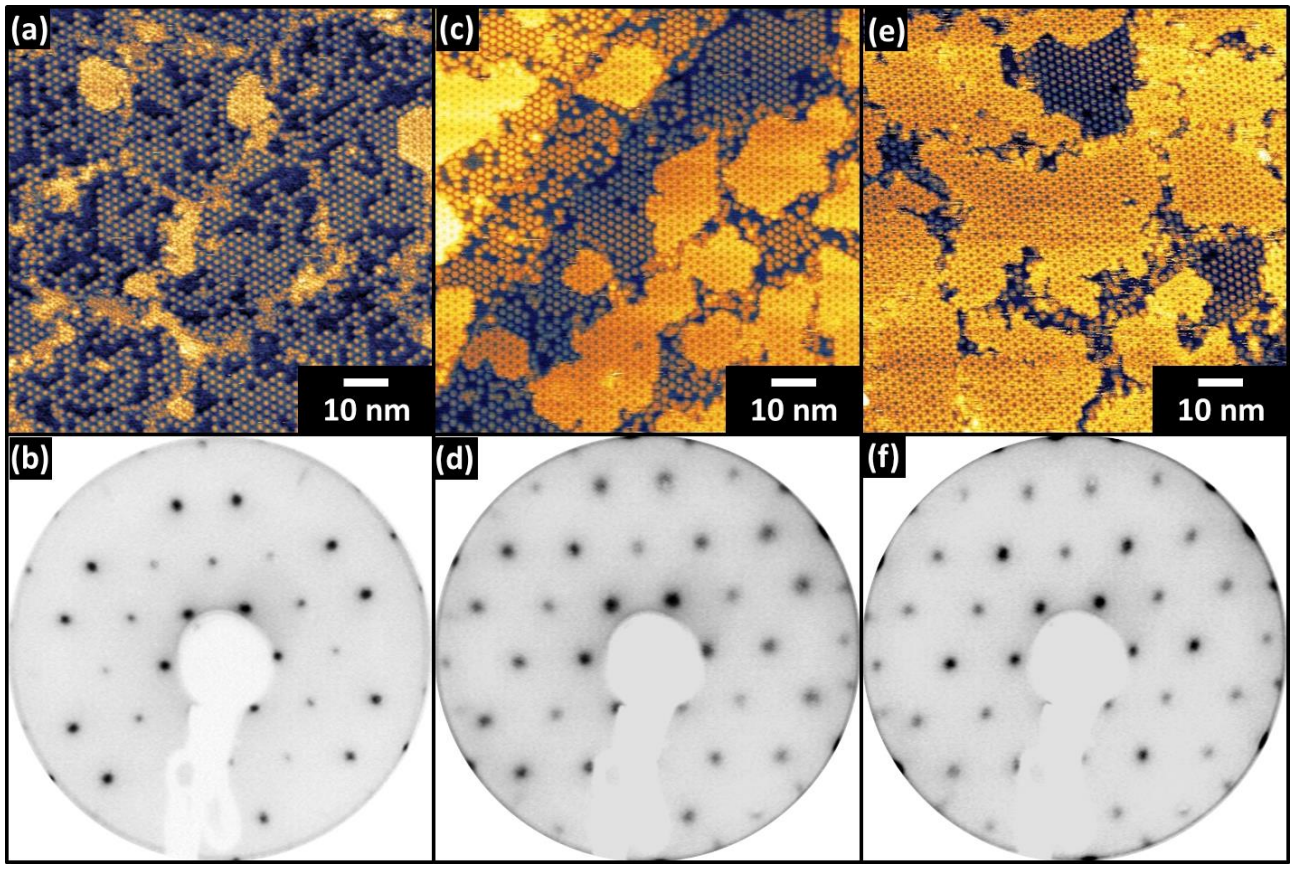

Figure 2 – STM images (all Vs=-1.65V, It=75pA) and corresponding LEED patterns (all 13eV) of low (a, b) medium (c,d) and high (e,f) coverages of C60 on truxenone (8x8)/Cu (111) surfaces.

observation of bilayers was surprising as the first C_{60} layer is not complete due to a seemingly random distribution of molecular vacancies. Some isolated molecules can be observed (lower middle) along with single molecular vacancies within the C_{60} domains of the first layer. This is indicative of the stability of individual molecules absorbed in the pores of the truxenone structure and precludes any hierarchical assembly process[23].

To ascertain whether or not bilayer growth was responsible for this observation, additional C_{60} was added to the surface in two stages. For intermediate coverages (Fig 2c,d), where the growth time was doubled, the areas of brighter contrast were more abundant and coexisted with monolayer regions. At higher coverage (Fig 2e,f), where the growth time was quadrupled, the brighter areas accounted for approximately 90% of the surface although monolayer regions were

still observed. This strongly suggests that the assertion that these regions are bilayers of C_{60} is correct, and indicates that bilayer formation was observed even without completion of the first C_{60} layer. Observation of this kind of growth indicates that adsorption of C_{60} onto the truxenone template and the first layer of C_{60} molecules is similarly energetically preferable.

The second layer of C_{60} molecules form a Kagome lattice[24] structure, something previously observed for C_{60} and C_{70} layers on porous molecular layers[25]. Although the authors have presented structural and energetic arguments for the formation and stabilisation of these structures, we believe that they are simply an expression of the same 8x8 symmetry as the first layer of C_{60} molecules. On close inspection every molecule in the second layer can be defined by a combination of 8x8 unit meshes. This is demonstrated schematically in Fig 3; panel (a) shows STM of monolayer and bilayer regions in the same area.

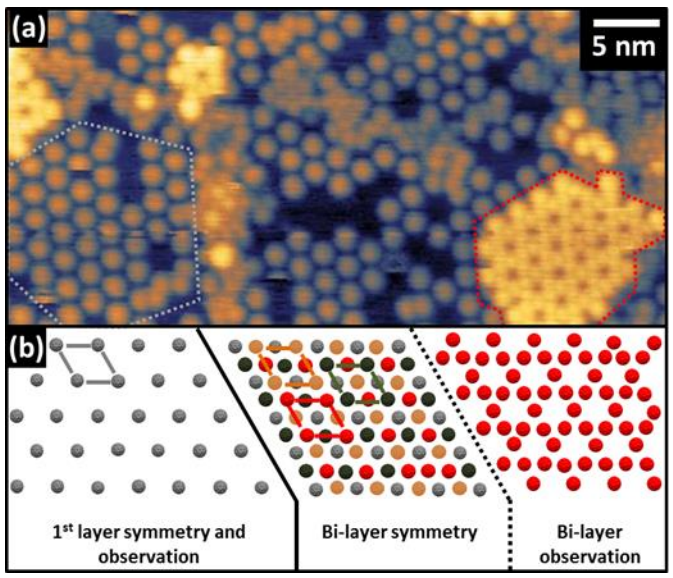

Figure 3 – STM image (V_s=1.5V, I_t=65pA) (a) of monolayer (white dashed box) and bilayer (red dashed box) regions. Panel (b) demonstrates three individual 8x8 meshes (separately coloured, unit cells marked) translated along the grey 8x8 mesh by half a unit cell along each of the primitive lattice directions to create the observed Kagome lattice.

In the left of panel (b) the symmetry of the first layer is depicted, the unit mesh marked by a grey rhombus. The middle panel shows the close-packed structure created by translating this mesh along each of its primitive translation vectors by half a unit cell length. If the underlying (first C_{60} layer) grey mesh is removed (to only consider the second layer) and the remaining three lattices are uniformly coloured, a pattern closely matching the observed bilayer visualisation is realised. This suggests that the second C_{60} layer is, in fact, a commensurate 8x8 structure despite initially appearing to have more complex symmetry. The observed Kagome lattice is formed by accommodation of three different 8x8 meshes on to a single underlying 8x8 C_{60} layer. A packing schematic considering the underlying truxenone lattice is included in supporting information (Figure S3).

These observations may explain the origin of Kagome lattices of C_{60} observed by other authors, but as previous studies did not include LEED data no direct comparison can be made. Although the periodicity of each LEED pattern is identical (i.e. the unit cell of the C_{60} and truxenone are the same) the intensity of the second and third order beams showed distinct differences. This indicates that although the C_{60} is templated into a lattice with common 8x8 *symmetry* the *surface structure* is not the same as the truxenone/Cu (111) 8x8.

In addition to templating the in-plane structure of the C_{60} layer the growth mode is also modified when compared with C_{60} grown on bare Cu (111). It is well documented in the literature that C_{60} on Cu (111) forms a 4x4 overlayer (confirmed by LEED patterns in Figure S4)[26,27]. STM images (Figure S4) show that C_{60} forms triangular three dimensional islands on Cu (111) with areas of exposed substrate remaining. The apparent size of C_{60} molecules in each layer of the multilayer structure is similar, and smaller than those in the first layer of the C_{60}/truxenone system.

The larger apparent size of the first layer of templated C_{60} molecules most probably results from geometric factors rather than electronic effects. The apparent lateral size of first layer molecules (approx. 2 nm, Figure S5) is likely increased by convolution of the molecular profile with the STM tip geometry, while the apparent size of those in the second (approx. 1 nm Figure S5) layer will be a more accurate representation of the distance between C_{60} molecules. In addition, first layer C_{60} molecules are likely to be mobile within the pores of the truxenone network in which they are captive. The rate of molecular motion is expected to be sufficiently high at room temperature that STM images represent an average of the position, resulting in larger apparent size. In both cases second layer C_{60} molecules would be expected to appear as smaller features than their first layer counterparts.

Further evidence is present in Figure 3, where C_{60} molecules at the edge of the red-dashed second layer region appear larger than those in the centre. Combined with isolated second layer molecules with almost identical apparent heights to molecules in the first layer, these observations preclude apparent height differences based on electronic effects.

Despite the difference in appearance the periodicity of first and second layers was identical as demonstrated by LEED patterns. These results demonstrate that epitaxial organic layers can be used to direct the epitaxial growth of multilayers of C_{60}. The formation of Kagome lattices is also observed in bilayers, and justified by the formation of multiple 8x8 lattices in the bilayer structures. The application of complementary surface imaging and diffraction allows the simple symmetry underlying complex visualisations to be revealed.

ASSOCIATED CONTENT

Supporting Information.

The following files are available free of charge.

Full experimental details, STM images and LEED patterns of C_{60} on Cu (111) (PDF)

AUTHOR INFORMATION

‡ Full experimental procedures are present in the supporting information

The authors declare no competing financial interests.

ACKNOWLEDGMENT

We acknowledge support from the Engineering and Physical Sciences Research Council [Grant Number EP/H021388/1]. The raw data associated with this article can be accessed at the following DOI: XXXXXXXX.

REFERENCES

(1) Yang, J.; Yan, D.; Jones, T. S. Molecular Template Growth and Its Applications in Organic Electronics and Optoelectronics. *Chem. Rev.* **2015**, *115* (11), 5570–5603.

(2) Slater, A. G.; Perdigão, L. M. A.; Beton, P. H.; Champness, N. R. Surface-Based Supramolecular Chemistry Using Hydrogen Bonds. *Acc. Chem. Res.* **2014**, *47* (12), 3417–3427.

(3) Ramadan, A. J.; Rochford, L. A.; Keeble, D. S.; Sullivan, P.; Ryan, M. P.; Jones, T. S.; Heutz, S. Exploring High Temperature Templating in Non-Planar Phthalocyanine/copper Iodide (111) Bilayers. *J. Mater. Chem. C* **2015**, *3* (2), 461–465.

(4) Slater (née Phillips), A. G.; Beton, P. H.; Champness, N. R. Two-Dimensional

Supramolecular Chemistry on Surfaces. *Chem. Sci.* **2011**, *2* (8), 1440.

(5) Sullivan, P.; Jones, T. S.; Ferguson, a. J.; Heutz, S. Structural Templating as a Route to Improved Photovoltaic Performance in Copper Phthalocyanine/fullerene (C[sub 60]) Heterojunctions. *Appl. Phys. Lett.* **2007**, *91* (23), 233114.

(6) Phillips, A. G.; Perdigão, L. M. A.; Beton, P. H.; Champness, N. R. Tailoring Pores for Guest Entrapment in a Unimolecular Surface Self-Assembled Hydrogen Bonded Network. *Chem. Commun.* **2010**, *46* (16), 2775-2777.

(7) Saywell, A.; Magnano, G.; Satterley, C. J.; Perdigão, L. M. A.; Champness, N. R.; Beton, P. H.; O'Shea, J. N. Electrospray Deposition of C 60 on a Hydrogen-Bonded Supramolecular Network. *J. Phys. Chem. C* **2008**, *112* (20), 7706–7709.

(8) Theobald, J. A.; Oxtoby, N. S.; Phillips, M. A.; Champness, N. R.; Beton, P. H. Controlling Molecular Deposition and Layer Structure with Supramolecular Surface Assemblies. *Nature* **2003**, *424* (6952), 1029–1031.

(9) Perdigão, L. M. A.; Perkins, E. W.; Ma, J.; Staniec, P. A.; Rogers, B. L.; Champness, N. R.; Beton, P. H. Bimolecular Networks and Supramolecular Traps on Au(111). *J. Phys. Chem. B* **2006**, *110* (25), 12539–12542.

(10) Räisänen, M. T.; Slater (née Phillips), A. G.; Champness, N. R.; Buck, M. Effects of Pore Modification on the Templating of Guest Molecules in a 2D Honeycomb Network. *Chem. Sci.* **2012**, *3* (1), 84–92.

(11) Bonifazi, D.; Enger, O.; Diederich, F. Supramolecular [60]fullerene Chemistry on Surfaces. *Chem. Soc. Rev.* **2007**, *36* (2), 390–414.

(12) Mena-Osteritz, E.; Bäuerle, P. Complexation of C60 on a Cyclothiophene Monolayer Template. *Adv. Mater.* **2006**, *18* (4), 447–451.

(13) Griessl, S. J. H.; Lackinger, M.; Jamitzky, F.; Markert, T.; Hietschold, M.; Heckl, W. M. Room-Temperature Scanning Tunneling Microscopy Manipulation of Single C 60 Molecules at the Liquid−Solid Interface: Playing Nanosoccer. *J. Phys. Chem. B* **2004**, *108* (31), 11556–11560.

(14) Pan, G.-B.; Cheng, X.-H.; Höger, S.; Freyland, W. 2D Supramolecular Structures of a Shape-Persistent Macrocycle and Co-Deposition with Fullerene on HOPG. *J. Am. Chem. Soc.* **2006**, *128* (13), 4218–4219.

(15) Yoshimoto, S.; Tsutsumi, E.; Narita, R.; Murata, Y.; Murata, M.; Fujiwara, K.; Komatsu, K.; Ito, O.; Itaya, K. Epitaxial Supramolecular Assembly of Fullerenes Formed by Using a Coronene Template on a Au(111) Surface in Solution. *J. Am. Chem. Soc.* **2007**, *129* (14), 4366–4376.

(16) Ramadan, A. J.; Nielsen, C. B.; Holliday, S.; Jones, T. S.; McCulloch, I.; Rochford, L. A. Organic/inorganic Epitaxy: Commensurate Epitaxial Growth of Truxenone on Cu (111). *RSC Adv.* **2016**, *6* (21), 17125–17128.

(17) Rochford, L. A.; Ramadan, A. J.; Holliday, S.; Jones, T.; Nielsen, C. The Effect of Fluorination on the Surface Structure of Truxenones. *RSC Adv.* **2016**.

(18) Nielsen, C. B.; Voroshazi, E.; Holliday, S.; Cnops, K.; Rand, B. P.; McCulloch, I. Efficient Truxenone-Based Acceptors for Organic Photovoltaics. *J. Mater. Chem. A* **2013**, *1* (1), 73–76.

(19) Nielsen, C. B.; Holliday, S.; Chen, H.-Y.; Cryer, S. J.; McCulloch, I. Non-Fullerene Electron Acceptors for Use in Organic Solar Cells. *Acc. Chem. Res.* **2015**, *48* (11), 2803–2812.

(20) Nielsen, C. B.; Voroshazi, E.; Holliday, S.; Cnops, K.; Cheyns, D.; McCulloch, I.

Electron-Deficient Truxenone Derivatives and Their Use in Organic Photovoltaics. *J. Mater. Chem. A* **2014**, *2* (31), 12348–12354.

(21) Yang, Z.-Y.; Tao, Y.; Chen, T.; Yan, H.-J.; Wang, Z.-X. Hydrogen Bonding Network of Truxenone on a Graphite Surface Studied with Scanning Tunneling Microscopy and Theoretical Computation. *Phys. Chem. Chem. Phys.* **2013**, *15* (6), 2105.

(22) Chen, F.; Hu, Z.; Ji, Y.; Zhao, A.; Wang, B.; Yang, J.; Hou, J. G. Interactions in Different Domains of Truxenone Supramolecular Assembly on Au(111). *Phys. Chem. Chem. Phys.* **2012**, *14* (11), 3980.

(23) Staniec, P. A.; Perdigão, L. M. A.; Saywell, A.; Champness, N. R.; Beton, P. H. Hierarchical Organisation on a Two-Dimensional Supramolecular Network. *ChemPhysChem* **2007**, *8* (15), 2177–2181.

(24) Atwood, J. L. Kagomé Lattice: A Molecular Toolkit for Magnetism. *Nat. Mater.* **2002**, *1* (2), 91–92.

(25) Wei, Y.; Reutt-Robey, J. E. Directed Organization of C 70 Kagome Lattice by Titanyl Phthalocyanine Monolayer Template. *J. Am. Chem. Soc.* **2011**, *133* (39), 15232–15235.

(26) Tamai, A.; Seitsonen, A. P.; Baumberger, F.; Hengsberger, M.; Shen, Z.-X.; Greber, T.; Osterwalder, J. Electronic Structure at the <math Display="“inline”> <msub> <mi mathvariant="“normal”">C</mi> <mn>60</mn> </msub> </math> /metal Interface: An Angle-Resolved Photoemission and First-Principles Study. *Phys. Rev. B* **2008**, *77* (7), 075134.

(27) Tatti, R.; Aversa, L.; Verucchi, R.; Cavaliere, E.; Garberoglio, G.; Pugno, N. M.; Speranza, G.; Taioli, S. Synthesis of Single Layer Graphene on Cu(111) by C 60 Supersonic Molecular Beam Epitaxy. *RSC Adv.* **2016**, *6* (44), 37982–37993.